Some MEMS Activities at the Jet Prepulsion Laboratory

Frank 'T'. Hartley

Jet Propulsion 1 aboratory
California Institute of Technology
4800 Oak Grove Drive, Pasadena CA 91109

Introduction

The Jet Propulsion Laboratory is a NASA Federally Funded Research and Development Center (FFRDC) which is endowed with NASA equipment that is managed and staffed by California Institute of 'T echnology with a highly educated and world class community of six thousand engineers and scientists. JPL's principal NASA responsibility is to design, build, test, and operate robotic spacecraft for the explorat ion of the solar system and to observe **our universe** across the whole EMR spectrum. Essentially, to go where no onc has gone before and in doing so determine the origins of our solar system and the universe.

Lofty stuff and, you might think, irrelevant to mere worldly endeavors of the MEMS industry. But robotic spacecraft must endure; the extreme temperatures of atmospheric entry and the almost absolute zero temperature of deep space; the vibration and moderate accelerations of launch and propulsion and the extreme retardation of impact penetrators; they must operate in dense corrosive atmospheres and in the hard vacuum of space; their performance can not be impaired by cosmic radiat ion and they must autonomously operate reliably for decades.

Capabilities

Ensuring survivability in such thermal and pressure regimes demands astute engineering, fastidious attention to detail, extensive modeling and definitive testing in environmental simulators. Mechanical robustness of complex mechanisms requires comparable endeavors from another group of engineers and testing in further simulators for acoustic noise (150 dB) and vibration loading under all orientations and acceleration spectrums.

The design of electronics resilient against radiation induced single event failures and latch up is another complex process as is the design of radiation shielding that addresses both primary and secondary radiation products. Radiation simulators arc needed to expose components and systems to maximum and integrated radiation dosages to determine life or failure probabilities. These capabilities reside at the Laboratory

JPL also operates a NIST traceable standards laboratory that provides comprehensive measurement calibration facilities for the testing of both ground support and flight instruments. The standards cover electromagnetic parameters; frequency and time; optical radiometry, pyrometry and photometry; thermodynam its; and mechanical mass, fore.c, pressure, vibration, shock , vacuum and flow. All necessary for successful flight systems.

The ensemble of environments that a space craft must endure encompass the smallest components, circuit modules, sub-system, instrument systems, and the whole spacecraft as well.

MEMS packaging design, fabrication and testing essentially represents a space craft microcosm where thermal, shock, atmosphere and radiation environments must be accommodated. The Technology Affiliates Program draws on its special competencies and facilities to undertake work for non-NASA government agencies and American industry contributing solutions to problems of national interest. Another industrial advantage of working with J] 'I, is that they operate under conditions of perpetual confidentiality and can not be commercial competitors.

Resources

Quality assurance is not just involved in the determination of classification ratings (i.e. Code S) for components and systems but in identifying the failure mechanisms and thereby identifying the path to improvement. Onc of the most useful non-destructive evaluation tools is the imaging scanning electron m icroscope. Even more useful arc 3D analysis, energy dispersive X-ray detection and electron back scatter imaging. The capital and maintenance cost of such equipment and the cost of experienced operators are beyond the budget of many M EMS fabrication companies. But not being able to identify contaminants or fabrication process anomalies could be the difference between success or failure of a MEMS manufacturing task.

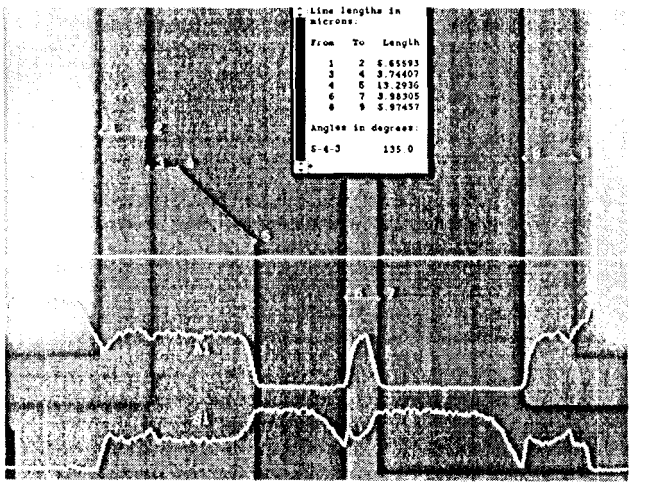

Figure 1 Structural Characterization

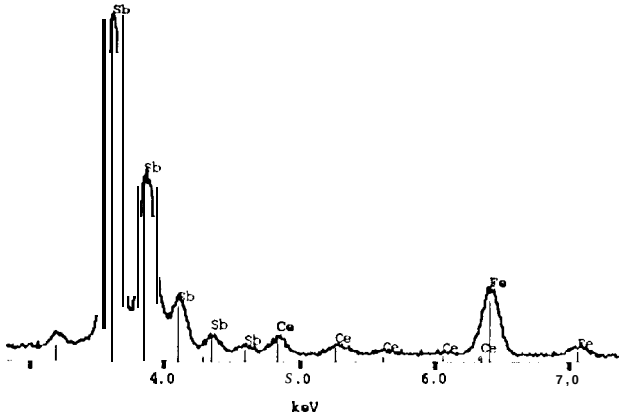

Figure 2 Energy Dispersive X-ray Spectrum

Figure 3 Secondary Electron Image

Structural characterization is useful (see Figure 1) in determining processed feature sizes, angles and shapes. One can imagine the further benefit of stereo or 3D structural characterization where the depth and orientation of etch, or presence of under cut etc. can be measured or identified. In contamination, deposition or etch analysis X-ray element spectroscopy is a very powerful tool. Figure 2 presents the element spatial resonances of the complete electron back scatter image presented in Figure 3, and Figures 4, 5 and 6 present element maps of each of the main constituents of Cesium (Cc), Antimony (Sb) and Iron (Fe) respectively.

Figure 4 X-ray Map of Cesium

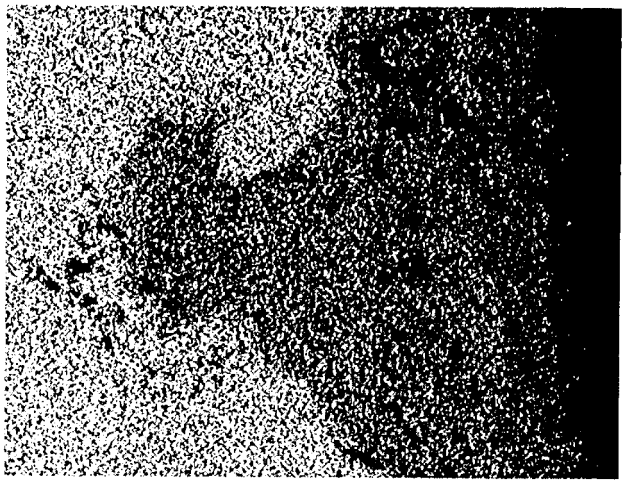

Figure S X-ray Map of Antimony

Figure 6 X-ray Map of Iron

In the nano-G accelerometer program the clement line scan version of this X-ray spectroscopy was most helpful in determining what the cause of interconnection continuity problems in the early fabrication process. The horizontal line across the middle of the spectral image in Figure 1 is such an elemental line scan and Figure 7 presents the elemental specificity along this line.

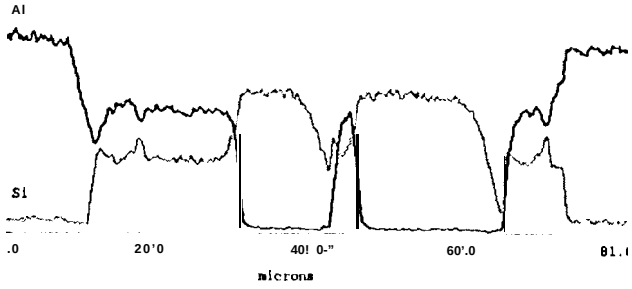

Figure 7 **Element** Specificity Along **Scan Line**

JPL also has a well equipped fabrication facility and an extensive MEMS program of its own as well &joint programs with other laboratories and universities. MEMS sensor manufacturing companies, having their own or leased fabrication facilities, would probably not have a need for JPL facilities per se although collaborative sensor developments are encouraged. JPL has developed many space and planetary related MEMS sensors which have been adapted to commercial applications, It is another JPL responsibility to transfer federally funded technology developments to American industry.

MEMS Sensors

By way of example, the evolution of a group of NASA funded MEMS programs and their potential for commercial exploitation will be discussed,

Nano-G Accelerometer

Under a NASA advanced technology development contract a nano-G accelerometer was developed in collaboration with Northeastern University. The intended use of the accelerometer was the tri-axial measurement of orbital drag on the Shuttle and Space Station where an acceleration range of $1o^{-2}$ - 10-8 G over a frequency range of 0.0001-25 Hertz were specified.

Silicon micromachined devices reported by others have not achieve the necessary sensitivity[i,ii]. These devices have been based on either piezoresistive or capacitive position sensing elements. The resolution of accelerometers is directly proportional to the position detection capability and the square of the fundamental frequency of the mechanical structure. Our accelerometer design is motivated by the need for small size and high sensitivity. For a low mass system this dictates ultra sensitive position detection such as that of an electron tunneling tip with an extreme spatial resolution of less than 0.001 Å/√Hz[iii,iv,v,vi,vii].

Three distinctively different dice arc fabricated during the process and arc subsequently assembled using an alloy bonding technique. Hermetic sealing and electrical connections between the different dice arc also accommodated during this bonding operation. The accelerometer is controlled by electrostatic force plates above and below the proof mass. The lower electrode has a dual role. In operation, it provides a necessary control electrode, and when not in operation, it is used to immobilize the proof mass to protect the flexures and particularly the tunneling tip.

The active clement (proof mass) of the accelerometer can be electrostatically suspended at the null position in a gravitation field by electrostatic levitation. The voltage to accomplish this is a function of the acceleration imposed upon the proof mass. This results in the elimination of one of the most serious difficulties in static and dynamic earth calibrations of micro G accelerometers. The same levitation feature permits the accelerometer to be nulled in a wide variety of conditions. The force actuation can provide an alternating excitation of the sensor to dynamically calibrate it over the frequency range of interest, In addition to both ground and in flight calibrations, this feature permits health monitoring, coefficient correction and sensor characterization over long term space flights.

A further important design issue for accurate tri-axial acceleration measurement is the minimization of off-axis sensitivity. This was accomplished by insuring that the proof mass and spring design was symmetric, weak in the compliant direction, and operated with the tunneling tip in close proximity to the unperturbed proof mass. As a consequence of a zero deflection flexure, thermal sensitivity is reduced, Thermal mismatched stress is also eliminated by fabricating all the die out of mono-crystalline silicon.

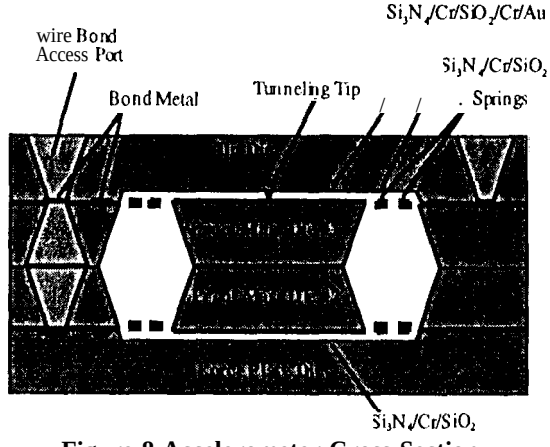

Figure 8 Accelerometer Cross Section

Figure 8 shows a not to scale cross section of the accelerometer indicating the important features of the four dice structure. 'I'he tip die (the top die in the figure) has an approximately 3.75 µm high tunneling tip at its center. Two identical proof mass dice are rotated by 180° are bonded together to form the 'proof mass'. The net weight of the proof mass is 0.18 gm which is held to the surrounding frame by a set of springs referred to as 'crab legs' and located in the exact center of the structure with the tunneling tip designed to just touch the unperturbed proof mass.

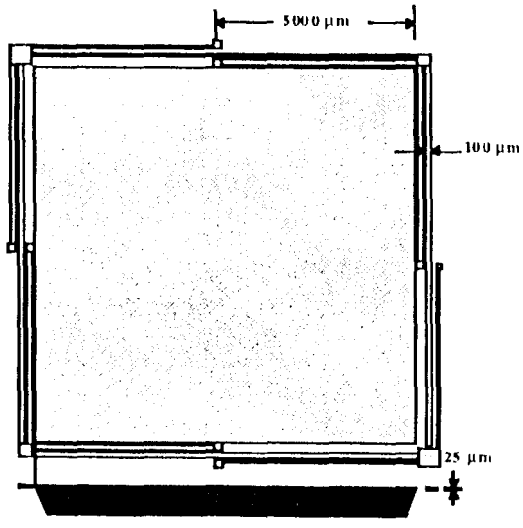

Figure 9 Partial Top View of Proof Mass

Figure 9 shows a portion of the top view of the proof mass and springs. Figure 10 shows a top view of the force plate die where the metal platen is covered with an oxide layer (0.5 μm) to prevent an electrical contact between the proof mass and the force plate when the proof mass is being electrostatically clamped.

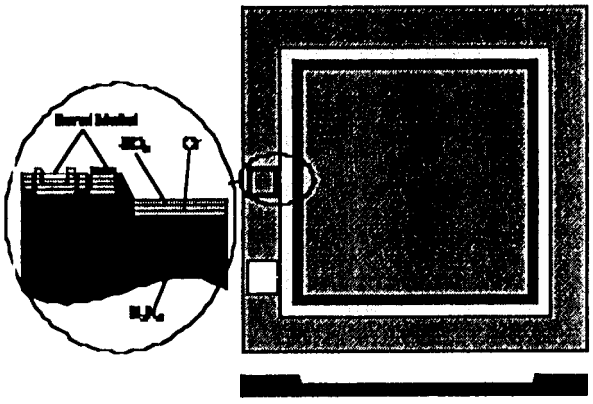

Figure IO Top View of Force Plate

Our bonding procedure is conducted at a low temperature (<400° C) which permits bonding, sealing and inter-connection after the wafers have been processed through metal deposition. Zero thickness referenced bonds are essential to maintain the tight spatial tolerancing required of this accelerometer. This eutectic bonding procedure was developed where etched channels were created in the bond regions (Figure 11) on which a spreading layer of metal was deposited and patterned in the channels. Finally the bond metal was deposited and patterned on top of the spreading layers in such a way that it protruded above the wafer surface and was narrower than the spreading layer such that it's volume was less than the volume of the channel. When two dice prepared in this way are brought in contact and heated, the bond metal melts and spreads by wicking and capillary forces reducing the spacing between the wafer surfaces to zero.

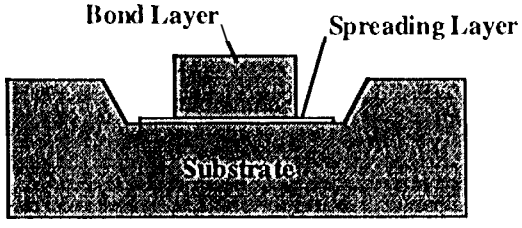

Figure 11Zero Thickness Eutectic Bonding

This sophisticated nano-G accelerometer was built and coupled with a de-sensitized 1-G controller. The seismic noise of the available terrestrial testing environment exceeded the resolution of the 1-G controller. However the sensitivity was determined to be sub micro-G and superior to the best of the commercial micro-G accelerometers (QA3000). Thermal dependence was not discernible and stability and accuracy were below the noise floor of the test system.

Coupled with a 10 mili-G controller this MEMS sensor is expected to meet it's design criteria of 10^{-2} - 10"8 G over a frequency range of 0.0001-25 Hertz. Further funding is being sought to undertake these conformation trials.

Aside from interest in the accelerometer by the international space faring nations there is interest from manufactures of active isolation systems. However the largest market is in sensitive seismometer-y and geological density gradient survey applications particularly down deep bore holes.

Enabling Technologies

The innovations that enabled the realization of this robust nano-G accelerometer are generic for a number of MEMS systems, specifically:

Zero thickness wafer bond.

Zero thickness bond means that the joining material is organized in such a way that an intimate contact of bare surfaces of joined wafers is possible. Thus, the spatial tolerancing alignment of the joint wafers is determined by the flatness of the wafers themselves, not the joining compound.

Encapsulation and wiring.

The developed wafer bonding techniques maintain vacuum inside the device. The modifications of the technique permit wafer to wafer electrical contacting or electrical isolation as desired.

Micromachined flexures.

The crableg flexure permit broad band independent adjustment of the in-plane and out-of-plane stiffnesses. the compliant axial mode and stiff pitch, roll and yaw mode deployed in the accelerometer ensures the parallel alignment of the elements.

Electrostatic 'caging'

Rc-deployable 'caging' can be sustained by a small battery during quiescent handling or during high acceleration or shock loading. Such a protective mechanism enables the deployment of flimsy structures and fragile tunneling tips in 'real world' sensors.

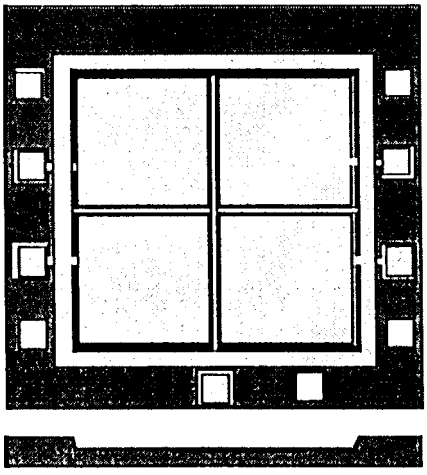

Figure 12 Tip-less Quad Plate

Active Optical Filter

The first derivative device under development is an active opt ical filter manufactured as an assembly of micromachined silica wafers. The wafers carry stationary and movable mirrors that form a reflective Fabry-Perot cavity. To make the device

feasible the mirrors must be aligned and keep their alignment. The position of the mirrors has to be controlled and measured while the geometry of the filters must not change with time or the environment.

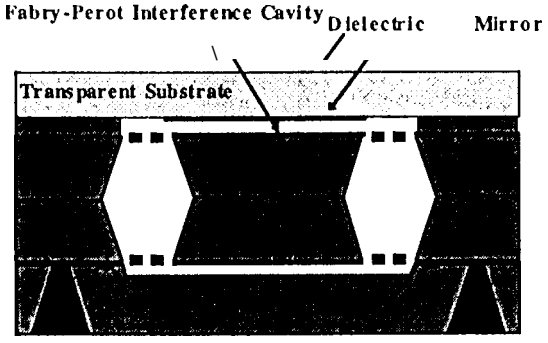

Figure 13 **Fabry-Perot Filter Cross Section**

In the reflective Fabry-Perot interferometer the proof mass and spring flexures of the accelerometer are used as a mirror platform to maintain surface parallelism accurately and constrain the cross-axial location of the movable mirror to the sub-pm level. The accelerometer tunneling tip is removed from the center quad plate (Figure 12) and the metal platens are covered with a thin insulation layer to facilitate 'caging' of the mirror. A thin metal layer is deposited on the lower surface of an opt ically flat transparent substrate followed by a dielectric mirror coating, The quad plate die, two proof mass dice and thin spacing dice are bonded together to form the adjustable cavity. Figure 13 illustrates how the dielectric coated mirror is placed over this cavity to produce a reflection Fabry-Perot cavity with the facing surface of the movable mirror (proof mass). The electrostatic platens on either side of the 'proof mass' face electrostatic platens on the quad die and behind the dielectric mirror enable monitoring and control of the spacing of the optical elements via capacitance measurement and force feedback through electrostatic actuators.

Such devices promise significant advantages in instrumentation for space astrophysics and quantitative imaging science in general and may become a major building block of the future opt ical imaging systems of microspacecraft, probes, and rovers.

One of the many potential applications of such a filter is to augment the Hubble Space Telescope (HST) advanced radial camera (WF/PC-III) spectral filter set. The use of ramp filters on WF/PC-I 1 has demonstrated the advantages of "tunable" filers. Fast moving objects can create very large red shifts. It is nearly impossible to provide a set of fixed filters that would cover all eventualities. The proposed tunable filter can provide complete spectral coverage and simultaneous imaging that is not possible with ramp filters. This capability will enable WF/PC-III to operate as an imaging spectrophotometer. Another major advantage ofa micro machined tunable filter is the lack of blue shift degradation that affects fixed filters. The Fabry-Perot based filter permits variable bandwidth, continuous tuning and a possibility of self-calibration It offers low weight, low energy consumption and an extreme thermal stability. The device has numerous commercial applications particularly as a multi color filter for camcorders and digital cameras.

Anemometer

The second derivative device under development is a sensitive anemometer for use on Mars to measure wind speeds of the low pressure CO_2 atmosphere. Here the proof mass of the accelerometer and its spring flexures are deployed not as a proof mass but as a large bathe plate that will be presented to the 'wind' and on which the pitot static force will apply.

The tipless quad platen is again used but with the center 50% of each of the quad plates removed as illustrated in Figure 14.

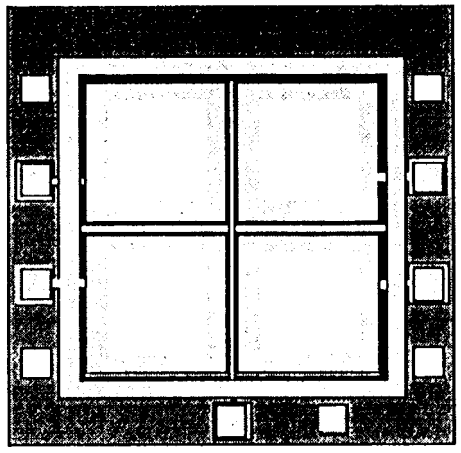

Figure 14 Perforated Quad Platens

The anemometer is then fabricated out of two baffle plates (proof mass) and two perforated quad dice eutectically bonded together as illustrated in Figure 15. Connections are then made to both baffle plates and each set of quad plates from both sides of the assembled unit.

During handling, launch etc., the baffle plate is clamped to either of the quad plates by means ofa small battery. The separation capacitance's of each quad plate, with respect to its' facing baffle plate, is measured and applied, via a control algorithm, to hold the baffle stationary in the center of the cavity, When the baffle is mounted perpendicular to the gas flow vector of interest the pitot static force (pressure x aperture area) applied from either side of the anemometer is determined from the aggregate voltages on each set of quad plates.

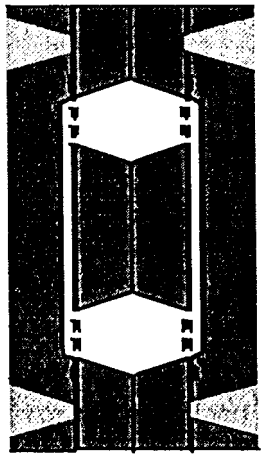

Figure1s Cross Section of Anemometer {NTS)

The micromachined anemometer dimensions are less than 2 cm square and 2 mm thick, it does not need to be mounted in a tube and two (or three) of them mounted orthogonaly (60°) will provide wind velocity. A unit mounted horizontally would provide a measurement of vertical drafts. The hi-polar force balanced arrangement of this anemometer provides for a wide dynamic range (1 O') and a bandwidth from sub-Hertz to hundreds of Hertz. The zero flexure deflection design and electrostatic actuator control ensure the anemometer is athermal and the relatively large baffle plates (0.5 cm^2) and compliant suspension ensure high sensitivity.

The commercial market for Martian anemometers would not be commercially compelling. } lowever the market for sensitive anemometers in industrial and domestic HVAC applications is large.

Derivative MEMS

These two derivative devices utilized the zero thickness bonding, encapsulation, wiring, micro flexures and electrostatic caging technologies spawned by the nano-G accelerometer development, The electrostatic 'caging' innovation also spawned the concept for an electrostatic peristaltic pump and inter wafer eutectic wiring spawned techniques for implementing ultra dense electronic circuit fabrication. These developments can not bc discussed in open forum but wc would be happy to discuss joint use opportunities with any organization that enters into a non-disclosure agreement.

Acknowledgments

The author acknowledges both NASA and JPL for their support of the MEMS programs and would like to thank Prof. Paul Zavracky, of Northeaster University, and Robert McClelland for their collaboration in the execution of these programs. James Kulleck's help in undertaking X-ray spectrometry work on the nano-G accelerometer and for providing some of the examples in this paper is also acknowledged,

E. Peeters, S. Vergote, B. Puers and W. Sansen, "A highly symmetrical capacitive micro-accelerometer with single degree of freedom response," J. Micromech. Microeng. Vol. 2, pp. 104-112, 1992.

Paper on ICSensor accelerometer.

T.W. Kenny, W.J. Kaiser, H.K. Rockstad, J.K. Reynolds, J.A. Podosek, and E.C. Vote, "Wide-Bandwidth Electromechanical Actuators for Tunneling Displacement Transducers," J. MEMS, Vol. 3, No. 3, September 1994.

T.W. Kenny, W.J. Kaiser, S.B. Waltman, and J.K. Reynolds, "A Novel Infrared Detector Based on a Tunneling Displacement Transducer," Appl. Phys. Lett, Vol. 59, 1991.

J.J. Yao, S.C. Arney, N.C. MacDonald, "Fabrication of High Frequency Two-dimensional Nanoactuators for Scanned Probe Devices," J. MEMS, Vol. 1, No. 1, pp. 14-22, 1992.

11. K. Rockstad, J. K Reynolds, T.K. Tang, T. W. Kenny, W. J. Kaiser, and T.B. Gabrielson, "A miniature, high-sensitivity, electron tunneling accelerometer," Transducers '95, pp 407 (PC 12).